Regenerative ability of augmented bone in rat calvarial guided bone augmentation model

Tatsuya Kubota

Nihon University Graduate School of Dentistry,

Major in Periodontology

(Directors: Prof. Shuichi Sato and Assist. Prof. Akira Hasuike)

Contents

The following article and new unpublished data (Fig. 2) are part of this doctoral thesis:

Regenerative capacity of augmented bone in rat calvarial guided bone augmentation model.

Tatsuya Kubota, Akira Hasuike, Yasumasa Ozawa, Takanobu Yamamoto, Katsuyoshi Tsunori, Yutaka Yamada, Shuichi Sato

Journal of Periodontal & Implant Science, Vol. 47, No. 2 (April, 2017)

Summary

Guided bone regeneration (GBR) is the most widely used technique to regenerate and augment bone. Even though augmented bone (AB) has been examined histologically in many studies, few studies have examined the biologic potential of AB and healing dynamics following its use. Further, it is unclear whether the bone obtained from a rat GBR procedure possesses functions on the same level as does the existing autogenous bone (AU). Therefore, the present study radiologically and histologically evaluated the regenerative capacity of AB in the occlusive space of rat guided bone augmentation (GBA) model.

The calvaria of five rats were exposed, and a plastic cap placed on the left side of the calvaria. Twelve weeks post-surgery, AB within the plastic caps were histologically evaluated. Twenty rats were randomly divided into two groups (AB and AU group) for primary surgery. For the 10 rats (AB group), the calvaria was exposed and a plastic cap was placed on the left side of the calvaria. In the remaining 10 rats (AU group), only skin incision and cutaneous flap elevation were performed in the same manner as performed in the AB group. Animals in the AU group were not placed plastic cap on the left side of the calvaria.

Secondary surgery was performed 12 weeks after the primary surgery. In all animals, a critical-sized calvarial bone defect (5.0 mm) was trephined into the dorsal bone on the right side. In the AB group, the plastic caps placed in the primary surgery were carefully removed, and regenerated bony tissue was harvested using a bone scraper. In the AU group, AU was harvested from the left side lateral bone in the rat calvarium using a bone scraper. After thoroughly rinsing the calvarial defects with physiological saline to wash out any bone fragments, the defects were filled with the previously harvested bone particles. In all animals, the skin was carefully sutured in the same manner as done in the primary surgery. Twelve

weeks post-surgery, critical sized bone defects were radiologically and histologically evaluated in both the AB and the AU groups.

Histological analysis revealed that the AB in the plastic cap showed almost the same mineralization as did the existing bone. In addition, more blood vessels, osteoblasts, and osteoclasts were observed in runt-related transcription factor 2 (RUNX2)-stained and tartrate-resistant acid phosphatase (TRAP)-stained sections. Analysis of the micro-CT images to measure bone volume (BV) indicated that the radiopacity contrast increased gradually and in a time-dependent manner in both groups. No significant difference was seen in BV between the AB and AU groups. In the micro-CT images of the AB and AU groups obtained at 0- and 4-week, many small radiopaque fragments were detected inside the defects. At 8 and 12-week, the number of radiopaque fragments produced by transplanted bone particles had decreased, and vigorous bone reossification at the edges of the bone defects was noted. Histological analysis revealed that the closure rates of the AB and the AU groups were not significantly different. The numbers of RUNX2- and TRAP-positive cells in the AB group was larger than those in the AU group.

From the result of this study, it was indicated that the regenerative ability of the AB particulate transplant was similar to that of the AU particulate transplant in critical-sized bone defects in rats. Therefore, AB could be used as an alternative to bone substitutes for implant treatment or other regeneration treatments.

Introduction

Dental implants are one of the best options for replacing missing teeth. As the demand for implant treatment continues to progress, there are many situations in which there is inadequate bone volume (BV) for the placement of dental implants. Guided bone regeneration (GBR) is the most widely used technique to regenerate and augment bone. A series of clinical studies [1-3] and animal experiments [4-6] have documented the effectiveness of GBR in augmenting bone.

The procedure of GBR was derived from the biological principle of "guided tissue regeneration" (GTR) developed by Nyman and Karring [7, 8] in the early 1980s for regenerating periodontal tissue lost as a result of periodontal disease. The principle of GTR was that the cells that first populated around wound area determine the type of tissue that ultimately occupies the space. Based on this principle, a technique utilizing barriers to prevent the migration of non-desirable epithelial cells into wounds was developed in the field of bone regeneration.

The sequence and pattern of bone regeneration in GBR procedures have been investigated in a few experimental studies [9-11]. Yamada et al. histologically studied GBR in rabbits with titanium caps placed on the calvarium [9, 10] and confirmed the presence of trabecular bone, consisting of mineralized bone and osteoid, bone marrow, and blood clots, in the occlusive space. Thus, the conclusions of this study indicated that the newly generated tissue in the occlusive space was considered to be bone tissue, augmented from the existing parietal bone. Schenk et al. [11] investigated surgically created, membrane-protected defects in the ridge in dogs, and they showed that healing started with the formation of a blood clot, which was replaced by a connective tissue matrix, then, deposited woven bone was replaced

by lamellar bone.

Even though augmented bone (AB) has been examined histologically in many studies [9, 10, 13, 14], however, a few studies have examined the biologic potential of AB and healing dynamics following its use. So, a question still remains whether the bone obtained from the GBR procedure possesses functions on the same level as does the existing autogenous bone (AU).

In the clinical conditions, it is still difficult to obtain an adequate quantity of AB for implant placement. To overcome these limitations, procedures using bone substitutes [12, 13] or bioactive molecules [14, 15] are used together with the original GBR theory. If the regenerative ability of AB is confirmed, the application of AB could be more widely used in regenerative surgery. Therefore, the purpose of present study was to histologically and radiologically evaluate the regenerative capacity of AB in rat GBA model.

Materials and Methods

Animals

Twenty-five eight-week-old male Fischer rats weighing 250-300 g were used. The animals were housed in an experimental animal room (22 ± 5°C, 55 ± 5% humidity, 12-/12- h light/dark cycle) and fed a standard laboratory diet and water. This study was approved by the Animal Experimentation Committee of the Nihon University School of Dentistry (AP14D026).

Rat GBA model

The rat GBA model reported and standardized previously [12, 13] was applied by setting plastic caps on the calvarium in five rats. The animals were premedicated by inhalation of isoflurane anesthetic and were subjected to general anesthesia by intraperitoneal injection of a mixture of 0.15 mg/kg dexmedetomidine hydrochloride, 2.0 mg/kg midazolam, and 2.5 mg/kg butorphanol tartrate. A local injection of 0.5 mL of a 1:80,000 dilution of lidocaine (Xylocaine; Astra Zeneca, Osaka, Japan) was administered to control bleeding and induce additional anesthesia.

Skin incisions approximately 6 cm long was made over the linea media to raise the skin of the calvarium. A cutaneous flap was raised laterally by using a small sharp periosteal elevator, and the periosteum was then incised and lifted to expose the calvarium. A circular groove was made on the left side of the midsuture using a trephine burr with an inner diameter of 5 mm under profuse irrigation with sterile saline. Five small holes were drilled with a No. 2 round burr to induce bleeding from the bone marrow space within each circle. The circular groove and five holes were created carefully so as not to penetrate the dura. Cylindrical plastic cap were pressed into the circular grooves and fixed in place with

light-cured four-methacryloyloxyethyl trimellitic anhydride resin.

Regenerative capacity of AB in rat calvarial bone defect model

Twenty rats were randomly divided into two groups (AB and AU group) for primary surgery. For the 10 rats in the AB group, anesthesia, incision, and flap elevation were performed in the same manner as for the GBA surgery. The calvarium was exposed and the plastic cap was placed on the left side of the calvarium. In the other 10 rats (AU group), only anesthesia, skin incision and cutaneous flap elevation were performed in the same manner. Animals in the AU group were not treated with the GBA procedure. In all animals, periosteum and skin were then carefully sutured with resorbable 4/0 polyglactin sutures.

Secondary surgery was performed 12 weeks after the primary surgery. In all animals, a critical-sized calvarial bone defect (5.0 mm) was trephined into the dorsal bone on the right side. Defects were created using a dental surgical drilling unit equipped with a trephine, which was constantly cooled with sterile saline. The calvarial disk was carefully removed to avoid tearing the dura. In the AB group, plastic caps placed in the primary surgery were carefully removed. Following this, regenerated bony tissue was harvested using a bone scraper (Safescraper, Osteogenics, Lubbock, TX, USA). In the AU group, AU was harvested from the left side lateral bone in the rat calvarium using a bone scraper. After thoroughly rinsing the calvarial defects with physiological saline to wash out any bone fragments, the defects were filled with the previously harvested bone particles. In all animals, the periosteum and skin were carefully sutured in the same manner as done in the primary surgery. The procedure performed in the AB group is demonstrated as schema (Fig. 1A), and a picture of the secondary surgery was taken just after removal of plastic caps (Fig. 1B).

Micro CT imaging analysis

Repeated micro-CT imaging was carried out using a micro-CT system (R_mCT2 system,

Tokyo, Japan) at 0, 4, 8, and 12-week post-surgery. Rats were anesthetized with inhalation of isoflurane and placed on the stage. Images of the regions of interest (ROI) were captured without euthanasia. The size of ROI was defined a diameter of 5.0 mm and a height of 3 mm. Bone tissue in the ROI was analyzed under the same conditions at each time point. The amount of BV within each ROI was examined using BV-measurement software (Kitasenjyu Radist Dental Clinic, I-View Image Center, Tokyo, Japan).

Histological analysis

Animals were sacrificed 12 weeks post-surgery by excess CO_2 gas inhalation. The skin was dissected and the defect sites were removed, along with the surrounding bone and soft tissues. Calvaria were harvested, fixed in 10% formalin, decalcified with a formic acid-sodium citrate decalcification solution for 1-week, and embedded in paraffin wax. Then, 5 μm-thick coronal sections through the center of the circular defect were prepared and processed for hematoxylin and eosin (HE) staining. Histological examination was performed under a light microscope equipped with a morphometric system, which was connected to a personal computer. From histological sections, defect closure rates (%) were calculated. Defect closure rate was determined by measuring the distance between the defect margins and was expressed as a percentage of the width of the total defect. Sections were deparaffinized, and endogenous peroxidase activity was quenched by incubation in 3% H_2O_2 in methanol at room temperature for 15 min. For the detection of osteoblasts, sections were incubated with human runt-related transcription factor 2 (RUNX2) antibodies (MBL Co., Tokyo, Japan) for 1 h. Secondary antibody staining was performed in accordance with the manufacturer's protocol. Immune complexes were visualized using 3'3'-diamibobenzidine tetrachloride (DAB; Merck, Darmstadt, Germany). Serial sections were also stained for tartrate-resistant acid phosphatase (TRAP), a marker of osteoclasts and osteoclast-like cells, as described previously [16]. Boxes

sized 5000 μm × 700 μm were virtually set in the central part of each defect. The mean numbers of RUNX2- and TRAP-positive cells in each box were counted in the central part of each defect.

Statistical analysis

Means and standard deviations were calculated for BV, closure rate, and the numbers of RUNX2/TRAP-positive cells. The Wilcoxon signed-rank test was used to analyze differences. The statistical analyses were performed using GraphPad Prism 5.0 (GraphPad software, La Jolla, CA, USA). The level of significance was set to 0.05.

Results

Healing progressed without complications in all animals. No sign of postoperative infection was observed in any experimental animal.

AB analysis

HE staining revealed that the AB in the plastic cap showed almost the same rate of mineralization as did the existing bone (Fig. 2A). In addition, RUNX2-stained and TRAP-stained AB sections had more blood vessels, osteoblasts, and osteoclasts than did sections derived from the existing bone (Figs. 2B, 2C).

Micro CT imaging analysis of the critical sized bone defect

Analysis of the micro-CT images measured as BV indicated that the radiopacity contrast increased gradually and in a time-dependent manner for both groups. Further, BVs were consistently kept at a much higher level from 0 to 12-week for both groups. No significant difference was seen in BV between AB and AU groups (Table 1).

Reossification developed by the extension of growth from the bony rims at the lateral sides of bone defects in all groups. In the AB and AU groups, the turning point of the healing process was confirmed as the time between 4 and 8-week post-surgery. In the micro-CT images of the AB and AU groups obtained at 0 and 4-week, many small radiopaque fragments inside the defects were detected. At 8 and 12-week, the number of radiopaque fragments produced by transplanted bone particles had decreased, and vigorous bone reossification in the edges of the bone defects was confirmed (Fig. 3).

Histological analysis of the critical-sized bone defect

HE staining confirmed bone reossification and defect closure tendency for both groups. (Figs. 4, 5). The defect closure rate was not significantly different in either AU or AB

groups (Table 2). In both groups, reossification were more vigorous on the dura side than on the periosteal site. In immunohistological analysis (for osteoblasts detection) of the AU group, a few RUNX2-positive osteoblasts were observed, and in that of the AB group, scattered RUNX2-positive osteoblasts were observed (Figs. 4B, 5B, and Table 2). Similar observations were noted in TRAP staining (for osteoclasts detection) of the two groups (Figs. 4C, 5C and Table 2).

Discussion

From the histological analysis showed that the AB in the plastic cap revealed almost the same mineralization as did the existing bone. Furthermore, more blood vessels, osteoblast-cells, and osteoclast-like cells were observed for the AB. Therefore, AB could possess regenerative ability and could be used as an alternative for AU in bone regeneration.

From the micro-CT analysis and histological analysis of AB and AU groups, it could be concluded that not only autogenous AU but also AB possess regenerative ability. Bone regeneration can be accomplished through three different mechanisms, namely, osteogenesis, osteoinduction, and osteoconduction [17, 18]. The bone obtained from AB particles could be more immature than AU and have active osteogenetic capacity. Consequently, more osteoblasts and osteoclasts were observed for the AB group than for the AU group. Therefore, osteogenesis capacity of the AB group at 12-week could be regarded as high.

The other factor related to healing in addition to the three regenerative components is "time" [19]. Indeed, the healing period is crucial for complete healing and bone regeneration. Histological analysis in the AB group at 12-week did not reveal sufficient defect closure. Since, cells were scattered in the histological sections derived from the AB group, it seem that bone healing and regeneration were still underway in 12 weeks, and the AB had active osteogenetic capacity. Thus, more advanced bone healing would be observed if the observation period is prolonged. Furthermore, the period between primary surgery and secondary surgery is also a very important factor. Further studies are required to demonstrate how these factors are related to the regenerative ability of GBA bone.

AU has been considered the gold standard because of its osteoinductive and conductive properties [20]. However, autogenous transplant cannot avoid the issues of limited

availability of samples and patient morbidity. Thus, GBR is thought to be a useful method to generate sufficient bone volume in which dental implants can be placed, making AB a valuable procedure. In the case of osteoplasty or drilling during implant placement preparation for AB, bone particles of AB could be generated. From This study suggests that AB has bone regenerative ability, and AB particles could be reused for regenerative purposes.

Conclusions

The regenerative ability of the AB particulate transplant was similar to that of the AU particulate transplant in critical-sized bone defects in rats. Therefore, AB could be used as an alternative to bone substitutes for implant treatment or other regeneration treatments.

Acknowledgements

This study was supported in part by a grant from Dental Research Center, Nihon University School of Dentistry for 2014.

References

1. Simion M, Trisi P, Piattelli A. Vertical ridge augmentation using a membrane technique associated with osseointegrated implants. Int J Periodontics Restorative Dent. 1994; 14: 496-511.

2. Tinti C, Parma-Benfenati S, Polizzi G. Vertical ridge augmentation: what is the limit? Int J Periodontics Restorative Dent. 1996; 16: 220-229.

3. Simion M, Jovanovic SA, Trisi P, Scarano A, Piattelli A. Vertical ridge augmentation around dental implants using a membrane technique and AU or allografts in humans. Int J Periodontics Restorative Dent. 1998; 18: 8-23.

4. Schmid J, Hämmerle CH, Stich H, Lang NP. Supraplant, a novel implant system based on the principle of guided bone generation. A preliminary study in the rabbit. Clin Oral Implants Res. 1991; 2: 199-202.

5. Linde A, Thorén C, Dahlin C, Sandberg E. Creation of new bone by an osteopromotive membrane technique: an experimental study in rats. J Oral Maxillofac Surg. 1993; 51: 892-897.

6. Jovanovic SA, Schenk RK, Orsini M, Kenney EB. Supracrestal bone formation around dental implants: an experimental dog study. Int J Oral Maxillofac Implants. 1995; 10: 23-31.

7. Nyman S, Gottlow J, Karring T, Lindhe J. The regenerative potential of the periodontal ligament. An experimental study in the monkey. J Clin Periodontol. 1982; 9: 257-265.

8. Nyman S, Lindhe J, Karring T, Rylander H. New attachment following surgical treatment of human periodontal disease. J Clin Periodontol. 1982; 9: 290-296.

9. Yamada Y, Nanba K, Ito K. Effects of occlusiveness of a titanium cap on bone generation beyond the skeletal envelope in the rabbit calvarium. Clin Oral Implants Res. 2003; 14: 455-463.

10. Yamada Y, Sato S, Yagi H, Ujiie H, Ezawa S, Ito K. Correlation in the densities of augmented and existing bone in guided bone augmentation. Clin Oral Implants Res. 2012; 23: 837-845.

11. Schenk RK, Buser D, Hardwick WR, Dahlin C. Healing pattern of bone regeneration in membrane-protected defects: a histologic study in the canine mandible. Int J Oral Maxillofac Implants. 1994; 9: 13-29.

12. Kochi G, Sato S, Ebihara H, Hirano J, Arai Y, Ito K. A comparative study of microfocus CT and histomorphometry in the evaluation of bone augmentation in rat calvarium. J Oral Sci. 2010; 52: 203-211.

13. Oginuma T, Sato S, Udagawa A, Saito Y, Arai Y, Ito K. AU with or without hydroxyapatite bone substitute augmentation in rat calvarium within a plastic cap. Oral Surg Oral Med Oral Pathol Oral Radiol. 2012; 114: S107-S113.

14. Shino H, Hasuike A, Arai Y, Honda M, Isokawa K, Sato S. Melatonin enhances vertical bone augmentation in rat calvaria secluded spaces. Med Oral Patol Oral Cirugí Bucal. 2016; 21: e122-e126.

15. Wen B, Li Z, Nie R, Liu C, Zhang P, Miron RJ et al. Influence of biphasic calcium phosphate surfaces coated with Enamel Matrix Derivative on vertical bone growth in an extra-oral rabbit model. Clin Oral Implants Res. 2016; 27: 1297-1304.

16. Hosoya A, Ninomiya T, Hiraga T, Zhao C, Yoshiba K, Yoshiba N et al. Alveolar bone regeneration of subcutaneously transplanted rat molar. Bone. 2008; 42: 350-357.

17. Misch CE, Dietsh F. Bone-grafting materials in implant dentistry. Implant Dent. 1993; 2: 158-167.

18. Giannoudis PV, Dinopoulos H, Tsiridis E. Bone substitute: an update. Injury. 2005; 36: S20–S27.

19. Wikesjö UM, Selvig KA. Periodontal wound healing and regeneration.Periodontology 2000. 1999; 19: 21-39.

20. Sakkas A, Wilde F, Heufelder M, Winter K, Schramm A. Autogenous bone grafts in oral implantology-is it still a "gold standard"? A consecutive review of 279 patients with 456 clinical procedures. Int J Implant Dent. 2017; 23: s40729-017-0084-4.

Figures

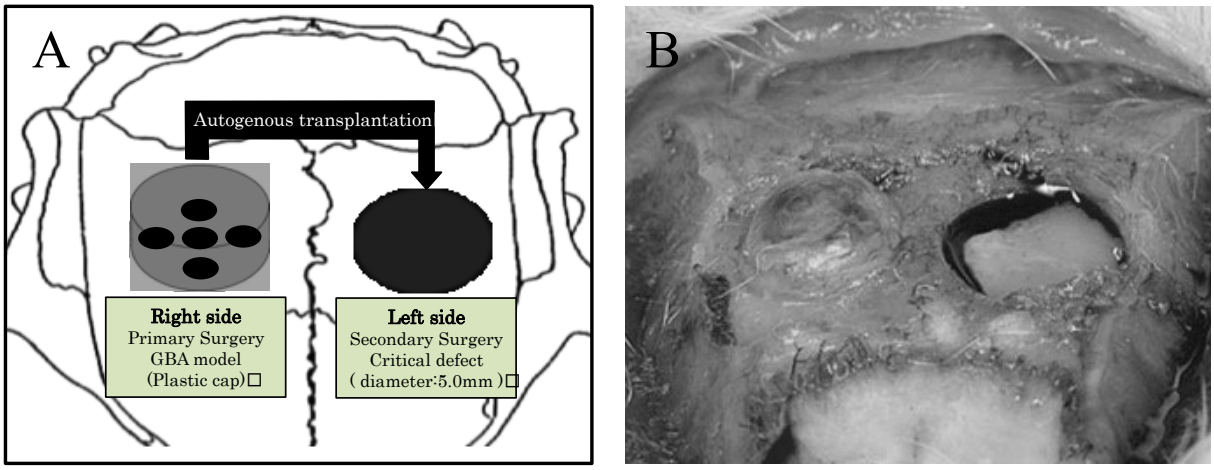

Fig.1: (A) Schematic of the AB group experimental model. (B) A picture from the secondary surgery of the AB group (right); critical defect creation on the left side was followed by plastic removal on the right side.

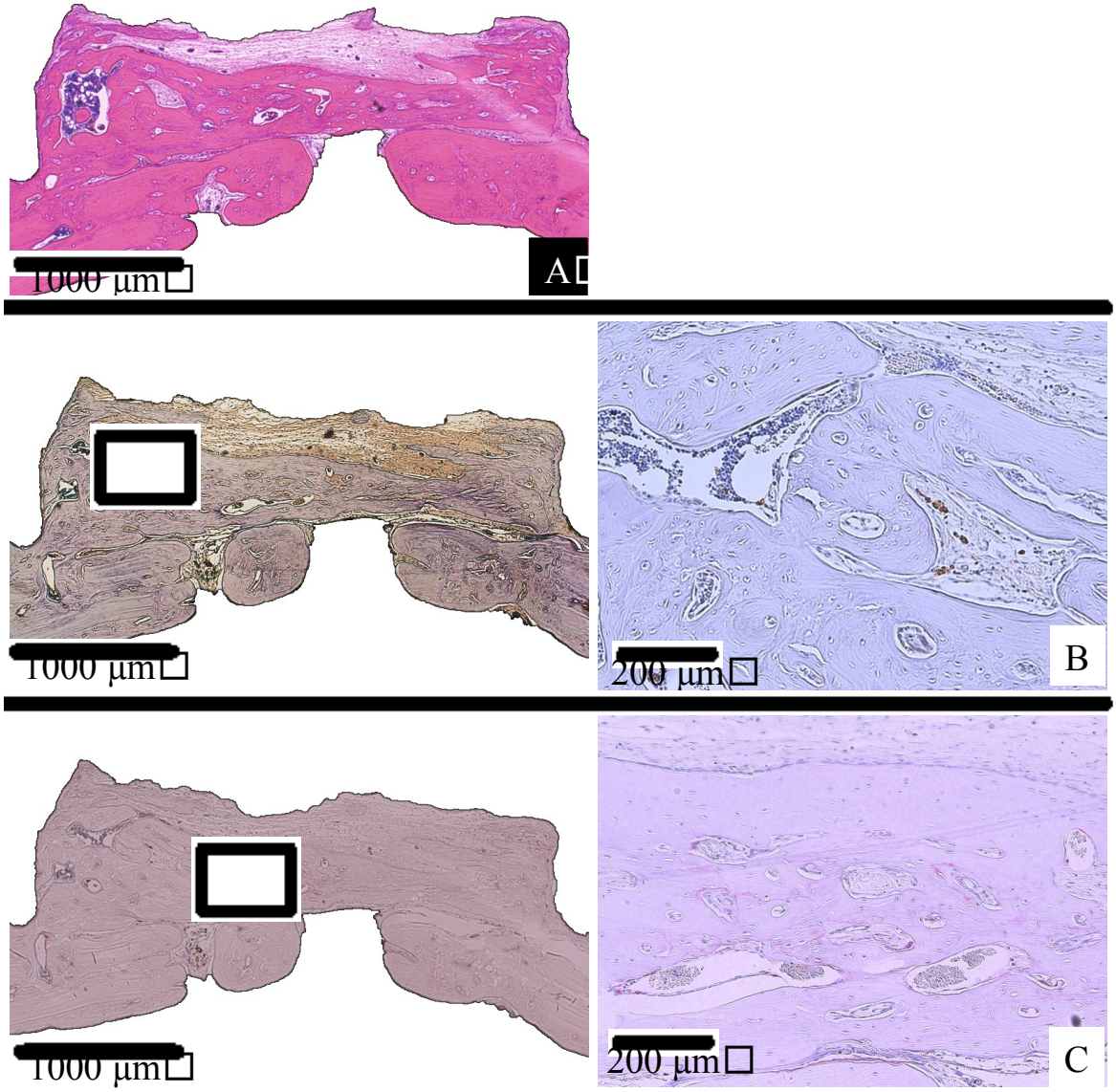

Fig. 2: Representative histological sections of the AB in the rat model of GBA.

A: HE-stained histological section

B: RUNX2-stained histological section

C: TRAP-stained histological section

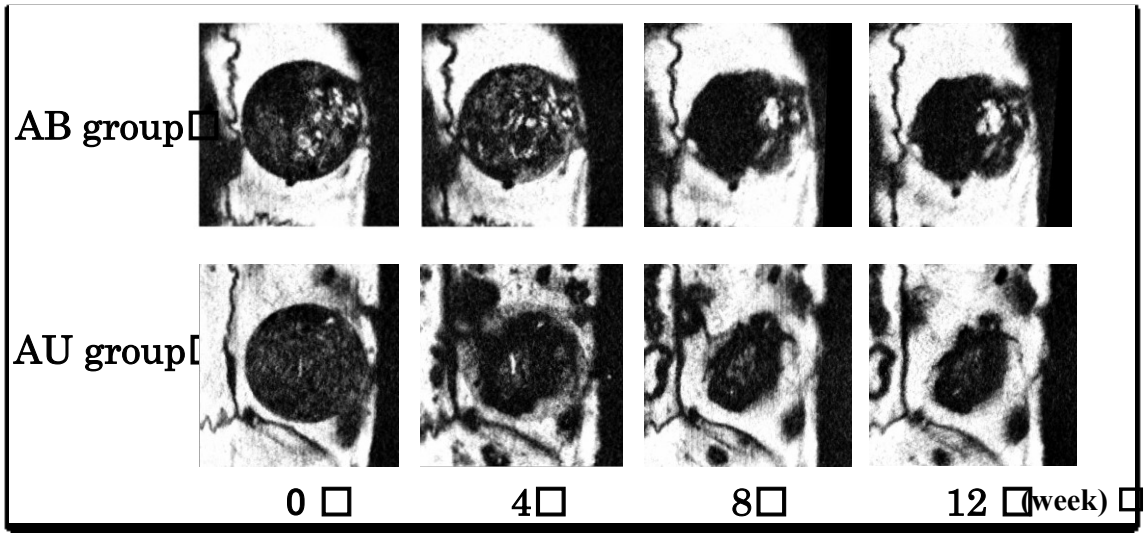

Fig. 3: Representative micro-CT image of critical defects in the AB and AU groups at 0, 4, 8, and 12-week after secondary surgery.

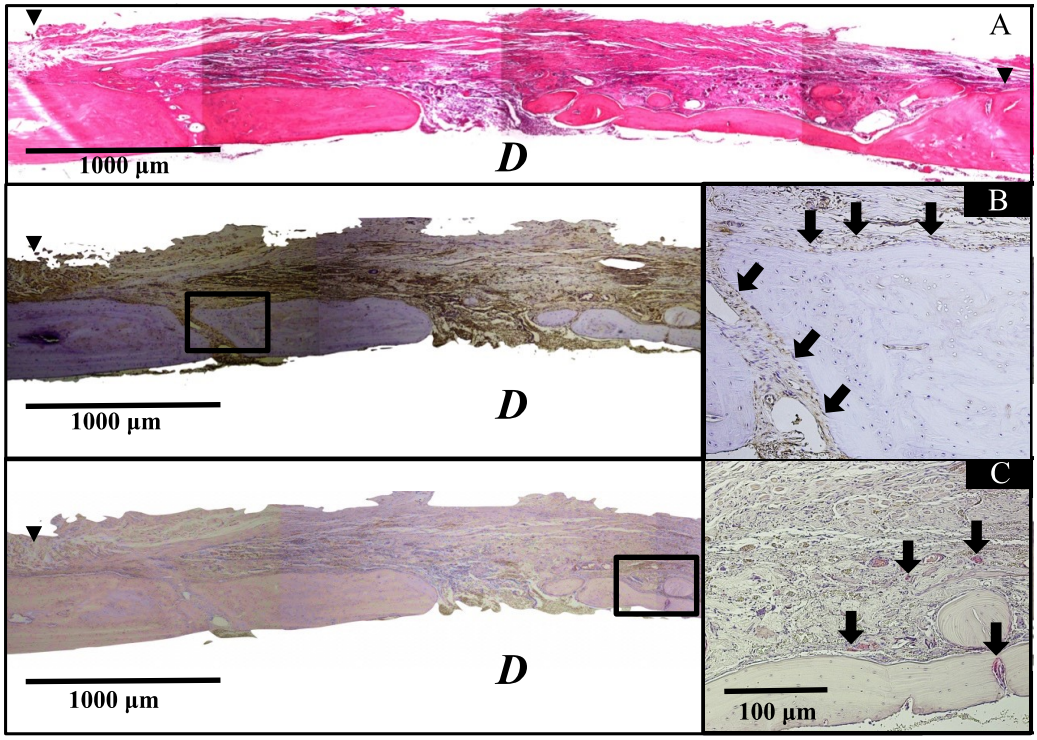

Fig. 4: Representative histological observation of the critical defects at 12 weeks in the AB group.

A: HE-stained histological section

B: RUNX2-stained histological section

C: TRAP-stained histological section

(⬇: positive reaction, *D* : dura side, ▼: edge of bone defect).

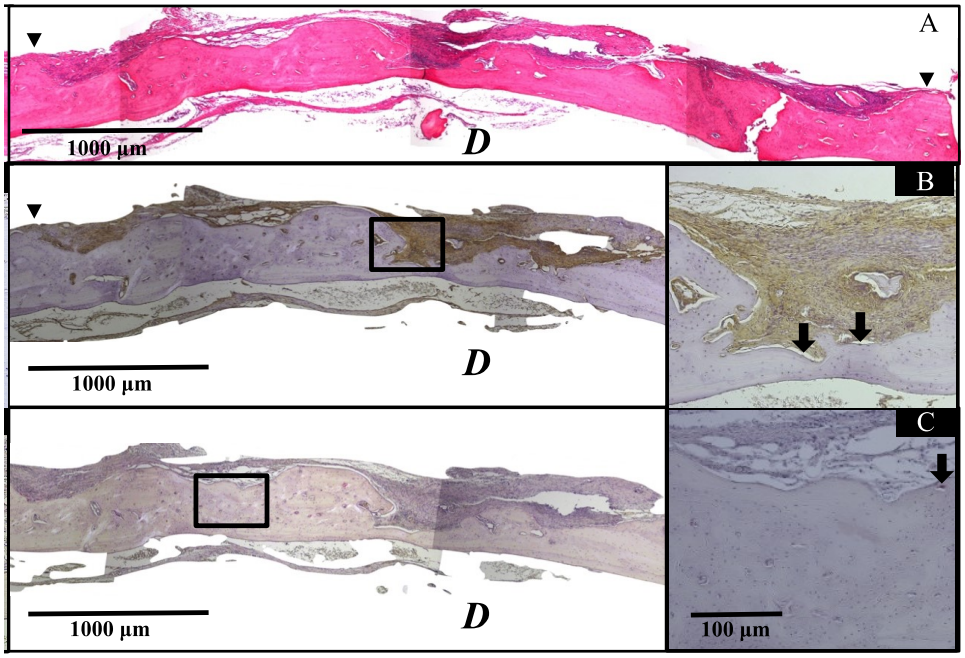

Fig 5: Representative histological observation of the critical defects at 12 weeks in the AU group.

A: HE-stained histological section

B: RUNX2-stained histological section

C: TRAP-stained histological section

(⬇: positive reaction, *D* : dura side, ▼: edge of bone defect).

Tables

Table 1. Results of bone volume (BV) in critical defects obtained from micro-CT (mean mm^3 ± SD).

Week	AB group	AU group
0	11.0 ± 1.3	9.9 ± 3.5
4	9.2 ± 3.0	8.9 ± 4.3
8	10.0 ± 3.5	10.1 ± 4.6
12	10.7 ± 4.2	10.5 ± 5.4

No signigficant difference (Wilcoxon signed-rank test)

Table 2. Results of histological bone defect closure rate and positive cell counting.

	AB group	AU group
Histological defect closure rate (%)	85.6 ± 15.8	91.3 ± 12.7
Number of Runx2 positive cells (cells)	280.9 ± 45.6 *	126.4 ± 34.5
Number of TRAP positive cells (cells)	43.9 ± 5.9 *	20.8 ± 4.1

*$P < 0.05$ (Wilcoxon signed-rank test)